

# Vision-Language Memory for Spatial Reasoning

Zuntao Liu<sup>1</sup>      Yi Du<sup>1</sup>      Taimeng Fu<sup>1</sup>      Shaoshu Su<sup>1</sup>      Cherie Ho<sup>2</sup>      Chen Wang<sup>1</sup>

<sup>1</sup>Spatial AI & Robotics (SAIR) Lab, University at Buffalo

<sup>2</sup>Stanford University

<https://sairlab.org/vlm2/>

## Abstract

*Spatial reasoning is a critical capability for intelligent robots, yet current vision-language models (VLMs) still fall short of human-level performance in video-based spatial reasoning. This gap mainly stems from two challenges: a semantic-geometric misalignment that prevents consistent 3D understanding, and the absence of persistent memory to retain 3D representation and understanding over time. To address these limitations, we present  $VLM^2$ , a Vision-Language Model with persistent Memory for spatial reasoning with a view-consistent, 3D-aware representation purely from 2D video. Specifically, to enhance long-horizon reasoning, we incorporate a dual-memory module, consisting of a working memory that operates as a sliding window to focus on immediate context, and an episodic memory that consolidates and stores critical long-term information. This design enables efficient and long-horizon spatial reasoning with a fixed computational cost. Extensive experiments on multiple benchmarks show that  $VLM^2$  achieves state-of-the-art performance among video-only models, significantly advancing the frontier of visual-spatial intelligence.*

## 1 Introduction

Spatial reasoning is a fundamental capability of intelligent robots, enabling them to perceive, localize, and reason about spatial relationships in the physical world. Recent advances [7, 14, 25, 37, 48, 74] have sought to enhance this ability in vision-language models (VLMs) [2, 30, 33, 36, 71], for instance by incorporating 3D information such as point clouds and depth maps to enhance spatial awareness. Despite these efforts, current video-based models still fall short of human-level spatial reasoning [6, 60]. There are two key underlying challenges in video-based spatial reasoning: (1) semantic-geometric feature misalignment and (2) absence of persistent memory. As shown in Figure 1, even a simple question “*How many chairs are there in this room?*” requires consistent cross-view alignment (recognizing the same chairs across different viewpoints and time steps) and long-horizon memorization (maintaining an ac-

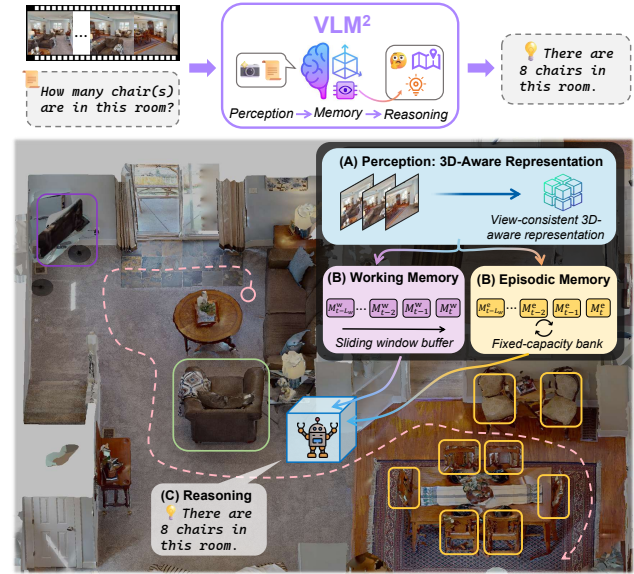


Figure 1.  $VLM^2$  is a Vision-Language Model with Memory for **long-horizon spatial reasoning** that constructs view-consistent 3D-aware representations from 2D video and maintains persistent memory over time. Such capabilities are critical for questions like “How many chairs are in this room?”, which require both consistent cross-view alignment and long-horizon memory.

curate count over time). However, existing methods often fail to address these two essential aspects simultaneously.

First, existing methods that leverage semantic features from 2D vision encoders tend to provide strong categorical understanding but lack precise metric grounding and positional awareness [15, 29, 65, 74], making it challenging to maintain spatial coherence across varying viewpoints. For instance, when moving from the living room to the kitchen, a model may incorrectly associate two distinct chairs at different locations as the same instance, resulting in spatial inconsistency. In contrast, geometric features derived from 3D visual geometry models offer reliable structural cues; however, naively fusing them with semantic representations often produces view-dependent instabilities [5, 34, 35, 43], causing global spatial inconsistencies under camera motion and making the model fail to understand the spatial scene.

The second challenge lies in the absence of persistent memory for diverse scenarios, although memory mechanisms have been explored in computer vision for decades [21]. Mobile robots often experience continuous viewpoint changes, partial observability, and frequent occlusions: objects may temporarily disappear and reappear as the viewpoint shifts [32, 57]. Existing VLMs [2, 33, 41, 71] rely on transient, token-based context windows that struggle to maintain a coherent, long-term spatial map [24, 62]. As new visual inputs arrive, previously observed information is easily overwritten or forgotten. For example, when a robot moves from the doorway to the kitchen and then returns, a chair initially seen at the entrance may no longer be recalled, leading to failures in long-horizon tasks such as object counting. This highlights the need for an explicit memory mechanism capable of persistently storing and updating 3D-aware representations across time and viewpoints.

To solve these challenges, existing approaches have explored several directions but with limited success. Early works [7, 14, 25, 37, 48, 74] fine-tuned VLMs with additional 3D data, but progress was constrained by the scarcity and limited diversity of such datasets. More recent methods [16, 54, 73] leverage geometric priors from 3D visual geometry foundation models [49–51], yet their reliance on simple feature fusion fails to resolve the semantic-geometric misalignment and lacks mechanisms for temporal persistence. As a result, these models are incapable of building a coherent representation of the 3D world.

In this paper, we present  $VLM^2$ , a **Vision-Language Model** with **persistent Memory** for spatial reasoning to construct a coherent long-term 3D memory of scenes. First, we construct a 3D-aware representation from video inputs by enforcing the alignment between the semantic and geometric features before fusion. To this end, we introduce a viewpoint-aware geometry alignment module to align geometry tokens with their view tokens, ensuring geometric features from different viewpoints are distinct even if their geometry is similar. Furthermore, we inject the predicted 3D coordinates into their corresponding visual tokens, ensuring the geometric awareness of visual tokens. To avoid potential spatial inconsistency, we introduce a learnable gate to decide which of these 3D points are useful, allowing the model to be “adaptive.” These design unlocks the model’s ability to perform spatial reasoning, yielding view-consistent 3D-aware representations under camera motion.

To equip with persistent memory, we introduce a dual-memory module that preserves and updates 3D-aware representations across time and viewpoints. It comprises (1) a working memory that functions as a sliding window over recent frames to capture immediate context, and (2) an episodic memory that serves as a fixed-capacity bank for long-term memorization. We design gated fusion and similarity-based update mechanisms to retain salient infor-

mation, recall previously observed objects, and maintain a coherent long-term spatial map for robust spatial reasoning. This design effectively mitigates the forgetting inherent to transient context windows, e.g., recalling a seen chair, while updating stored representations to remove redundancy, keeping computation and storage bounded. We note that 3DLM-Mem [24] is a concurrent effort to enhance memorization in VLMs. However, its unpruned memory accumulates redundant entries and incurs high computation on long videos. In contrast, our dual-memory design integrates a sliding-window working memory for recent context with a fixed-capacity episodic memory that performs gated fusion, preserving salient observations while enabling bounded yet persistent long-horizon reasoning.

We evaluate  $VLM^2$  on multiple spatial reasoning and 3D understanding benchmarks, including VSI-Bench [60], VSTI-Bench [16], ScanQA [1], and SQA3D [40].  $VLM^2$  achieves superior performance among video-only models and surpasses open-sourced VLMs and spatial-enhanced models [2, 16, 54, 72, 73], advancing the frontier of visual-spatial intelligence. Our main contributions include:

- We introduce a vision-language model for spatial reasoning, integrating a semantic-geometric consistent representation with a persistent dual-memory, enabling coherent spatial reasoning from video.  $VLM^2$  achieves state-of-the-art performance on multiple benchmarks, including VSI-Bench, VSTI-Bench, ScanQA, and SQA3D.
- We develop a 3D-aware representation for spatial reasoning that resolves semantic-geometric misalignment by adaptively grounding visual features into 3D space and enforcing cross-view consistency to ensure coherent and consistent 3D understanding. We also design a dual-memory module that couples a sliding-window working memory with a fixed-capacity episodic memory, achieving persistent yet efficient long-horizon spatial reasoning.

## 2 Related Work

### 2.1 3D Large Language Models

Recent efforts have focused on enabling 3D large language models to understand 3D scenes by introducing explicit 3D modalities [7, 8, 22, 26, 27, 48, 53, 74, 75]. Early work LL3DA [7] employs a point cloud encoder for scene-level representations, while Chat-3D [53], LEO [27], and Chat-Scene [26] segment objects and aggregate object-level 3D features for scenes. 3D-LLM [22] recovers 3D cues from rendered multi-view images via a 3D feature extractor, while LLaVA-3D [75] injects 3D position to form 3D-aware patch aggregation. More recently, Video-3D LLM [74] encodes 3D position into the visual representation. Ross3D [48] leverages reconstruction-based supervision to learn 3D-aware features. GS-Reasoner [8] constructs a 3D scene representation by integrating geometric features extracted from a point cloud encoder. These ap-

proaches improve 3D understanding, yet they rely on explicit 3D inputs (e.g., point clouds, depth maps). In contrast, our framework learns 3D-aware representations from 2D video, requiring no additional 3D data or supervision.

## 2.2 Spatial Reasoning in VLMs

Equipping VLMs with spatial reasoning capabilities has recently emerged as a significant area of research [4, 6, 12, 39, 44, 59, 61]. However, previous work has mainly focused on spatial understanding from 2D static images, leaving video-based spatial reasoning as a relatively underexplored domain. To address this gap, VSI-Bench [60] introduces a video-based benchmark to evaluate how effectively VLMs can understand spatial relationships. Recent studies [16, 29, 54, 73] have further sought to enhance VLM spatial reasoning by incorporating geometric priors from 3D Visual Geometry Foundation Models (VGFMs). For instance, Spatial-MLLM [54] and VG-LLM [73] leverage VGFMs (e.g. VGGT [49]) as spatial encoders to extract geometric features. Similarly, 3DRS [29] introduces supervision signals from pretrained VGFMs, although this approach relies on additional 3D data to compute position information. VLM-3R [16] incorporates implicit 3D tokens from pretrained VGFMs (e.g., CUT3R [50]) and further proposes the VSTI-Bench to evaluate the comprehension of spatial relationships evolving over time. Despite these advances, a common limitation of these methods is their tendency to simply fuse geometric features with semantic cues. Without explicitly addressing the potential semantic-geometric misalignment, their performance improvements remain constrained. In contrast, our work introduces an explicit alignment mechanism to learn a view-consistent 3D-aware representation, which more effectively integrates semantic and geometric cues for spatial reasoning.

## 2.3 Memory for Spatial Reasoning

Memory mechanisms have been adopted in vision tasks that depend on long-range temporal or spatial information. Their applications include video understanding [19, 45, 67], video generation [28, 55, 64], and 3D reconstruction [11, 47, 56]. This paradigm has also been explored for life-long navigation in embodied agents [31], where memory representations are critical. Within this embodied context, several works focus on building spatial memories. For instance, MTU3D [77] maintains a dynamic spatial memory bank for grounding and exploration, while 3D-Mem [62] constructs a 3D scene memory from multi-view images for exploration and reasoning. More recently, 3DLM-Mem [24] equips 3D LLMs with long-term memory to support diverse embodied tasks. However, this approach has notable limitations: it requires explicit 3D inputs, and its unpruned memory accumulates redundant entries and incurs high computational cost on long videos. In contrast, our work operates in a video-only setting and introduces a

bounded dual-memory module to address these challenges. This module couples a sliding-window working memory with a fixed-capacity episodic memory, preserving salient information for persistent yet efficient spatial reasoning.

## 3 Method

### 3.1 Overview

We introduce  $VLM^2$ , a vision-language model that takes as input a monocular video  $\mathcal{V} = \{I_t\}_{t=1}^N$  and a language instruction  $Q$ , and generates answers by using a persistent memory built from view-consistent 3D-aware representations. An overview of our architecture is shown in Figure 2. Our method is built on two key innovations. First, to address semantic-geometric misalignment, we explicitly align visual, geometry, and view tokens into a view-consistent 3D-aware representation (Sec. 3.2) that maintains spatial consistency under camera motion. Second, building on this consistent 3D-aware representation, we introduce a dual-memory module (Sec. 3.3) that equips  $VLM^2$  with persistent memory for both immediate and long-term context. This enables the model to reason about spatial layouts and objects no longer in view, supporting long-horizon spatial reasoning. We implement  $VLM^2$  on top of LLaVA-Video [72]. The 3D-aware, memory-enhanced representations are concatenated with the instruction embeddings and fed into the language backbone to generate answers.

### 3.2 View-Consistent 3D-Aware Representation

Given a video, the goal is to produce a view-consistent, globally coherent 3D-aware representation built from varying viewpoints, in which local semantic and geometric information is aligned for improved spatial reasoning. First, we uniformly sample  $N$  frames  $\{I_t\}_{t=1}^N$  from the input video, where  $I_t \in \mathbb{R}^{H \times W \times 3}$ . From each frame  $I_t$ , we extract visual tokens  $F_t \in \mathbb{R}^{h \times w \times c}$  capturing semantic information from a pretrained vision encoder, and geometric priors from a 3D foundation model ( $\pi^3$  [52]): geometry tokens  $G_t \in \mathbb{R}^{h \times w \times c_g}$ , view tokens  $Z_t \in \mathbb{R}^{h \times w \times c_v}$ , and per-pixel point maps  $X_t \in \mathbb{R}^{H \times W \times 3}$ . However, directly fusing these features suffers from a core semantic-geometric misalignment: the visual tokens  $F_t$  lack spatial grounding, while the geometry tokens  $G_t$  are viewpoint-ambiguous. We introduce three core modules to address this issue: (1) *Adaptive 3D Position Injection* injects predicted 3D coordinates into visual tokens while handling noisy predictions; (2) *Viewpoint-Aware Geometry Alignment* aligns geometry tokens with their corresponding view tokens to resolve view ambiguity; and (3) *Semantic-Geometric Fusion* fuses these aligned features into a 3D-aware representation that enables spatial reasoning consistent across camera motion.

**Adaptive 3D Position Injection.** While recent works, such as Video-3D LLM [74], achieve improved spatial awareness by injecting 3D position information into visual tokens. However, they require additional 3D data, such as ground-

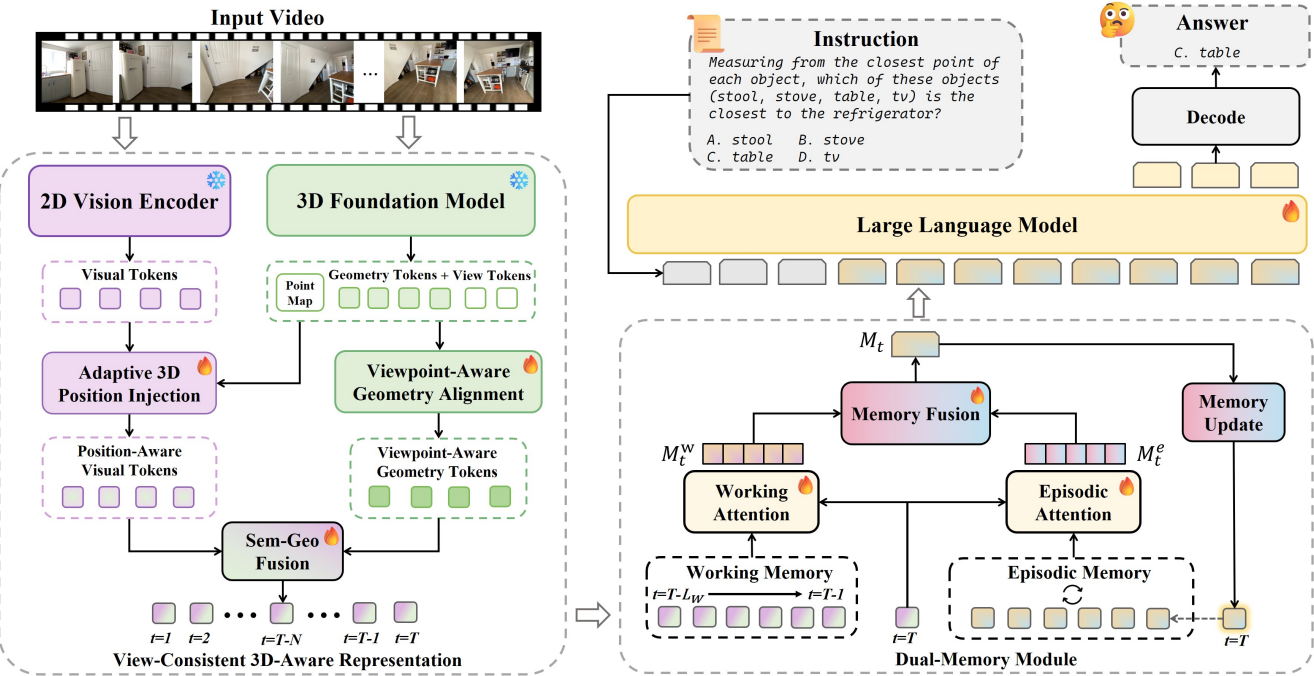


Figure 2. **Overview of the VLM<sup>2</sup> Architecture.** Our model constructs a view-consistent 3D-aware representation via adaptive 3D position injection, viewpoint-aware geometry alignment and semantic-geometric fusion. A dual-memory module with a sliding-window working memory and a fixed-capacity episodic memory maintains these representations over time, supporting long-horizon spatial reasoning.

truth depth maps and camera matrices. We leverage a 3D foundation model to predict point maps  $X_t$ . However, uniformly injecting all predicted 3D coordinates degrades performance due to noise and inaccuracies in the predictions. To address this, we introduce an adaptive gating mechanism that selectively incorporates reliable and useful 3D position cues (e.g. chairs instead of walls) while filtering out noisy or irrelevant predictions. We first obtain per-patch 3D coordinates  $C_t \in \mathbb{R}^{h \times w \times 3}$  by pooling the point maps  $X_t$ , then encode them into 3D position embeddings  $C'_t \in \mathbb{R}^{h \times w \times c}$  via a sinusoidal position encoding and a two-layer MLP  $\phi: \mathbb{R}^3 \rightarrow \mathbb{R}^c$ . The core of our adaptive design is a learnable gate  $\alpha_t$  that modulates the injection:

$$F_t^{\text{pa}} = F_t + \alpha_t \odot \phi(C_t), \quad \alpha_t \in [0, 1]^{h \times w \times 1}, \quad (1)$$

where  $\odot$  denotes element-wise multiplication. This produces position-aware visual tokens  $F_t^{\text{pa}}$  that are grounded in 3D, while mitigating the impact of prediction noise.

**Viewpoint-Aware Geometry Alignment.** Direct fusing visual and geometric features presents a crucial challenge: the geometric features alone are viewpoint-ambiguous (e.g., a chair’s front and back legs produce similar features). To make the geometric feature viewpoint-aware, we infuse geometry tokens with both patch-level and frame-level perspective cues. First, to disambiguate local geometric patterns, we enrich geometry tokens with the corresponding view tokens, projected via a linear layer  $\psi_v: \mathbb{R}^{c_v} \rightarrow \mathbb{R}^{c_g}$

produce  $\hat{Z}_t$ . This fusion produces viewpoint-aware features  $G_t^{\text{va}}$  that make patch-level geometry less ambiguous.

$$G_t^{\text{va}} = \text{MLP}(\text{Concat}[G_t; \hat{Z}_t]). \quad (2)$$

Second, to provide global viewpoint context, we append a global view descriptor  $\bar{Z}_t \in \mathbb{R}^{1 \times 1 \times c_v}$ , obtained by pooling view tokens  $Z_t$  and projecting through a linear layer  $\psi_g: \mathbb{R}^{c_v} \rightarrow \mathbb{R}^{c_g}$ . This provides a frame-level signal of the camera’s overall viewpoint direction.

$$G_t^{\text{vc}} = \text{Concat}[G_t^{\text{va}}; Z_t^g] \in \mathbb{R}^{(hw+1) \times c_g}. \quad (3)$$

Infused with both patch-specific and frame-level viewpoint information, the resulting geometric tokens  $G_t^{\text{vc}}$  are now viewpoint-aware across different viewpoints.

**Semantic-Geometric Fusion.** To form the final 3D-aware representation for each frame  $I_t$ , we fuse the position-aware visual tokens and viewpoint-aware geometry tokens through cross-attention. We use the position-aware visual tokens  $F_t^{\text{pa}}$  as queries and the viewpoint-aware geometry tokens  $G_t^{\text{vc}}$  as keys and values:

$$H_t = \text{Attn}(Q(F_t^{\text{pa}}), K(G_t^{\text{vc}}), V(G_t^{\text{vc}})). \quad (4)$$

The output  $H_t$  is a sequence of powerful 3D-aware tokens for frame  $I_t$  that bind visual semantics to consistent geometric structure, resolving the semantic-geometric misalignment and producing a coherent 3D-aware representation that supports reliable spatial reasoning across views.

---

**Algorithm 1** Dual-Memory Module

---

**Input**  $H_t, \mathcal{W}_t, \mathcal{E}_t$   
**Output**  $M_t, \mathcal{W}_{t+1}, \mathcal{E}_{t+1}$

- 1:  $\triangleright$  **Working Retrieval**
- 2:  $M_t^w \leftarrow$  Working Attention( $Q = H_t, KV = \mathcal{W}_t$ )
- 3:  $\triangleright$  **Episodic Retrieval**
- 4:  $M_t^e \leftarrow$  Episodic Attention( $Q = H_t, KV = \mathcal{E}_t$ )
- 5:  $\triangleright$  **Gated Memory Fusion**
- 6:  $\gamma_t = \sigma(\text{MLP}(\text{Concat}[M_t^w; M_t^e]))$
- 7:  $M_t = \gamma_t \odot M_t^w + (1 - \gamma_t) \odot M_t^e$
- 8:  $\triangleright$  **Update Working Memory**
- 9: **if**  $|\mathcal{W}_t| < L_w$  **then**
- 10:    $\mathcal{W}_{t+1} \leftarrow \mathcal{W}_t \cup \{H_t\}$
- 11: **else**
- 12:   **remove** oldest element from  $\mathcal{W}_t$
- 13:    $\mathcal{W}_{t+1} \leftarrow \mathcal{W}_t \cup \{H_t\}$
- 14: **end if**
- 15:  $\triangleright$  **Update Episodic Memory**
- 16: **if**  $|\mathcal{E}_t| < L_e$  **then**
- 17:    $\mathcal{E}_{t+1} \leftarrow \mathcal{E}_t \cup \{M_t\}$
- 18: **else**
- 19:   **for**  $i = 1$  **to**  $L_e$  **do**
- 20:      $s_i \leftarrow \cos(M_t, E_i)$
- 21:   **end for**
- 22:    $i_t^* \leftarrow \arg \max_{i \in \{1, \dots, L_e\}} s_i$
- 23:   **del**  $E_{i_t^*}$ ;  $\mathcal{E}_{t+1} \leftarrow \mathcal{E}_t \cup \{M_t\}$
- 24: **end if**
- 25: **return**  $M_t, \mathcal{W}_{t+1}, \mathcal{E}_{t+1}$

---

### 3.3 Dual-Memory Module

Inspired by CUT3R [50], which maintains a continuously updating state for 3D reconstruction, we propose a dual-memory module that stores and updates 3D-aware representations. This enables long-term spatial memory, mitigating catastrophic forgetting in long-horizon tasks.

**Working Memory for Immediate Retrieval.** An agent’s immediate environment is dense with information, but not all recent observations are equally relevant. To dynamically focus on important short-term context, we design a sliding-window working memory  $\mathcal{W}_t$  to store the most recent  $L_w$  representations. Our key insight is that the model should retrieve only what is relevant rather than treating all recent information equally. We achieve this selective retrieval by using the current representation  $H_t$  as queries to attend over the working memory’s content via cross-attention:

$$M_t^w = \text{Attn}(Q(H_t), K(\mathcal{W}_t), V(\mathcal{W}_t)). \quad (5)$$

The resulting feature  $M_t^w$  is an enhanced representation of the current state, enriched with the most relevant context from the immediate past and recent observations.

**Episodic Memory for Long-Horizon Recall** While the working memory captures relevant recent context, it can-

not retain crucial information over long horizons, making it difficult to perform spatial reasoning requiring long-term recall. For instance, the chair counting example in the introduction requires retrieving observations that may no longer be in the sliding window. To overcome this, we introduce an episodic memory  $\mathcal{E}_t = \{E_1, E_2, \dots, E_{L_e}\}_{i=1}^{L_e}$ , a fixed-capacity bank that stores the most salient observations. The model implicitly learns what constitutes a “task-relevant” memory through end-to-end training on QA tasks, guiding it to preserve representations useful for spatial reasoning. Similar to the working memory, we use the current representation  $H_t$  to query episodic memory via cross-attention, yielding an episodic-enhanced representation  $M_t^e$ .

**Memory Fusion and Update.** The working-enhanced representation  $M_t^w$  is fused with the episodic-enhanced representation  $M_t^e$  to produce the final memory-enhanced feature for the current step. We employ a learnable gate  $\gamma_t$  to control the combination of these two information streams:

$$\gamma_t = \sigma(\text{MLP}(\text{Concat}[M_t^w; M_t^e])), \quad (6)$$

$$M_t = \gamma_t \odot M_t^w + (1 - \gamma_t) \odot M_t^e. \quad (7)$$

This produces the final memory-enhanced representation  $M_t$ . To maintain a diverse and non-redundant episodic memory bank, we replace the most similar existing entry with current memory-enhanced representation  $M_t$ . Specifically, we identify the most similar entry  $E_{i_t^*}$  in episodic memory and update it with the new representation  $M_t$ .

$$i_t^* = \arg \max_{i \in \{1, \dots, L_e\}} \cos(M_t, E_i). \quad (8)$$

This similarity-based update mechanism ensures episodic memory remains bounded, diverse, and rich with salient information, enabling long-horizon spatial reasoning.

## 4 Experiments

**Implementation Details.** Our model is built on LLaVA-Video-7B [72], a video LLM based on Qwen2-7B [46], and uses  $\pi^3$  [52] as the 3D foundation model. We train for one epoch on a mixed dataset using the same learning objective as VLM-3R [16]. We use the AdamW optimizer with a batch size of 128 and a peak learning rate of 1e-5 for the LLM during the warmup phase. For fine-tuning, we apply Low-Rank Adaptation (LoRA [23]) with a rank of 128 and a scaling factor of 256. Both the vision encoder and 3D foundation model are kept fully frozen during training. All experiments are conducted on 8 NVIDIA H200 GPUs.

### 4.1 Spatial Reasoning Benchmarks

**Datasets and Metrics.** We evaluate our model’s spatial reasoning performance on VSI-Bench [60], which contains over 5,000 QA pairs collected from egocentric videos in ScanNet [13], ScanNet++ [63], and ARKitScenes [3]. To assess persistent spatial reasoning over time, we adopt VSTI-Bench [16], which is built on the same video sources

Table 1. **Evaluations on VSI-Bench [60] for 3D spatial reasoning tasks.** We compare against proprietary models, open-sourced VLMs, and spatial-enhanced models specifically designed for spatial reasoning. Bold indicates the best performance.

Methods	Rank	Avg.	Numerical Qusetion				Multiple-Choice Question			
			Obj. Cnt.	Abs. Dist.	Obj. Size	Room Size	Rel. Dist.	Rel. Dir.	Route Plan	Appr. Order
<i>Proprietary Models (API)</i>										
GPT-4o	3	34.0	46.2	5.3	43.8	38.2	37.0	41.3	31.5	28.5
Gemini-1.5 Flash	2	42.1	49.8	30.8	53.5	54.4	37.7	41.0	31.5	37.8
Gemini-1.5 Pro	1	45.4	56.2	30.9	64.1	43.6	51.3	46.3	36.0	34.6
<i>Open-sourced VLMs</i>										
LongVA-7B	10	29.2	38.0	16.6	38.9	22.2	33.1	43.3	25.4	15.7
InternVL2-8B	6	34.6	23.1	28.7	48.2	39.8	36.7	30.7	29.9	39.6
InternVL2-40B	4	36.0	34.9	26.9	46.5	31.8	42.1	32.2	34.0	39.6
LongVILA-8B	12	21.6	29.1	9.1	16.7	0.0	29.6	30.7	32.5	25.5
VILA-1.5-8B	11	28.9	17.4	21.8	50.3	18.8	32.1	34.8	31.0	24.8
VILA-1.5-40B	9	31.2	22.4	24.8	48.7	10.7	40.5	25.7	31.5	32.9
Qwen2.5VL-7B	7	33.0	40.9	14.8	43.4	10.7	38.6	38.5	33.0	29.8
Qwen2.5VL-72B	3	37.0	25.1	29.3	54.5	38.8	38.2	37.0	34.0	28.9
LLaVA-OneVision-7B	8	32.4	47.7	20.2	47.4	12.3	42.5	35.2	29.4	24.4
LLaVA-OneVision-72B	2	40.2	43.5	23.9	57.6	37.5	42.5	39.9	32.5	44.6
LLaVA-NeXT-Video-7B	5	35.6	48.5	14.0	47.8	24.2	43.5	42.4	34.0	30.6
LLaVA-NeXT-Video-72B	1	40.9	48.9	22.8	57.4	35.3	42.4	36.7	35.0	48.6
<i>Spatial-Enhanced Models</i>										
VG-LLM-4B	5	47.3	66.0	37.8	55.2	59.2	44.6	45.6	33.5	36.4
VG-LLM-8B	3	50.7	67.9	37.7	58.6	62.0	46.6	40.7	32.4	59.2
Spatial-MLLM-4B	4	48.4	65.3	34.8	63.1	45.1	41.3	46.2	33.5	46.3
VLM-3R-7B	2	60.9	70.2	49.4	69.2	67.1	65.4	80.5	45.4	40.1
<b>VLM<sup>2</sup>-7B (Ours)</b>	<b>1</b>	<b>68.8</b>	<b>72.5</b>	<b>59.6</b>	<b>70.8</b>	<b>69.9</b>	<b>69.0</b>	<b>87.8</b>	<b>52.6</b>	<b>68.3</b>
<i>Improve ↑</i>	-	+7.9	+2.3	+10.2	+1.6	+2.8	+3.6	+7.3	+7.2	+28.2

and comprises approximately 6,000 QA pairs. This benchmark evaluates not only on 3D environment understanding from input video but also on reasoning about cameras, objects, and their evolving relationships over time. For Multiple-Choice Answer (MCA) tasks, we report standard *Accuracy* [17, 20, 66], and for Numerical Answer (NC) tasks, we report *Mean Relative Accuracy* [60].

**Baselines.** We compare our model with a diverse set of proprietary and open-source VLMs (e.g., GPT-4o [30], Gemini-1.5 Pro [18], LLaVA-NeXT-Video [71], Qwen2.5-VL [2]). We also include recent spatial-enhanced models for spatial reasoning, including SPAR [68], VG-LLM [73], Spatial-MLLM [54], and VLM-3R [16].

**Results on VSI-Bench.** Table 1 presents the quantitative results on VSI-Bench. Our method consistently outperforms proprietary and open-source VLMs across all task categories on VSI-Bench. The performance gains are particularly pronounced on *Absolute Distance* and *Relative Direction*, as these tasks demand strong spatial awareness and fine-grained 3D understanding. This suggests that our model learns view-consistent and spatially-aware representations that effectively capture geometric cues. Moreover, our method attains state-of-the-art results on *Route Plan* and *Appearance Order*. The former emphasizes long-horizon spatial reasoning, while the latter requires spatial understanding over time, further demonstrating that our dual-memory module retains key information over long horizons.

Table 2. **Evaluations on VSTI-Bench [16] for 3D spatial-temporal reasoning tasks.** Abbr.: CO-AbsD = Cam-Obj Abs. Dist.; CDisp = Cam. Displace.; CMDir = Cam. Mov. Dir.; OO-RelP = Obj-Obj Rel. Pos.; CO-RelD = Cam-Obj Rel. Dist. Bold indicates best performance in each model category.

Methods	Avg.	Numerical Question		Multiple-Choice Question		
		CO-AbsD	CDisp	CMDir	OO-RelP	CO-RelD
<i>Proprietary Models (API)</i>						
GPT-4o	38.2	29.5	23.4	37.3	58.1	42.5
Gemini-1.5 Flash	32.1	28.5	20.9	24.4	52.6	33.9
<i>Open-sourced VLMs</i>						
LongVA-7B	32.3	13.5	5.1	43.7	57.9	41.2
InternVL2-8B	43.5	32.9	13.5	48.0	68.0	55.0
InternVL2-40B	43.2	11.9	34.9	33.3	63.8	72.2
LongVILA-8B	30.5	20.0	11.6	35.4	52.3	33.4
VILA-1.5-8B	37.3	30.1	27.3	42.2	50.4	36.7
VILA-1.5-40B	38.2	28.2	15.7	28.8	65.4	53.0
Qwen2.5VL-7B	38.2	22.9	4.9	47.4	65.9	49.9
Qwen2.5VL-72B	40.3	18.0	10.0	41.0	74.2	58.4
LLaVA-OneVision-7B	41.7	29.9	19.3	47.5	62.1	49.8
LLaVA-NeXT-Video-7B	40.0	28.2	1.8	49.8	64.7	55.6
LLaVA-NeXT-Video-72B	44.0	32.3	10.5	48.1	78.3	50.9
<i>Spatial-Enhanced Models</i>						
VLM-3R-7B	58.8	39.4	39.6	60.6	86.5	68.6
<b>VLM<sup>2</sup>-7B (Ours)</b>	<b>65.3</b>	<b>43.1</b>	<b>44.1</b>	<b>76.8</b>	<b>87.7</b>	<b>74.9</b>
<i>Improve ↑</i>	+6.5	+3.7	+4.5	+16.2	+1.2	+6.3

**Results on VSTI-Bench.** As shown in Table 2, we evaluate our model’s capability for persistent spatial reasoning over time on VSTI-Bench. Our method achieves state-of-the-art performance across all tasks, with an overall accuracy of 65.3, a relative improvement of 11.1% over the previous

Table 3. **Long-horizon spatial reasoning performance on VSI-Bench [60] and VSTI-Bench [16].** Videos are grouped into Short (< 1 min), Mid (1–2 min), and Long (> 2 min).

Methods	VSI-Bench				VSTI-Bench			
	Avg.	Short	Mid	Long	Avg.	Short	Mid	Long
VLM-3R-7B	63.2	67.1	64.7	60.0	63.6	61.1	64.7	66.4
<b>VLM<sup>2</sup>-7B (Ours)</b>	<b>69.4</b>	<b>71.0</b>	<b>70.0</b>	<b>68.1</b>	<b>69.5</b>	<b>65.9</b>	<b>70.6</b>	<b>74.6</b>
<i>Improve</i> $\uparrow$	+6.2	+3.9	+5.3	+8.1	+5.9	+4.8	+5.9	+8.2

best method VLM-3R (58.8), reflecting consistent gains on both spatial and temporal reasoning categories. We attribute these gains to the combination of our 3D-aware representation, which provides a stable and view-consistent spatial understanding, and our persistent memory, which maintains this understanding coherently over time.

**Analysis on Long-Horizon Reasoning Abilities.** To evaluate the long-horizon spatial reasoning ability of the models, we partition the input videos in VSI-Bench [60] and VSTI-Bench [16] into three groups based on their duration: Short (< 1 min), Mid (1–2 min), and Long (> 2 min). Table 3 shows the comparisons. On VSI-Bench, VLM-3R’s performance clearly degrades as video length increases, suggesting that it struggles to retain and integrate spatial information over long sequences. On VSTI-Bench, while VLM-3R’s performance remains relatively stable across different lengths, our model consistently achieves higher accuracy, with the largest gains on long videos. Overall, VLM<sup>2</sup> improves the average accuracy by +6.2 and +5.9 points on VSI-Bench and VSTI-Bench, respectively, with the largest gains on long videos. These results demonstrate that our view-consistent 3D-aware representation and dual-memory design effectively preserve spatial understanding over long horizons, highlighting the importance of persistent memory for reliable long-horizon spatial reasoning.

## 4.2 3D Scene Understanding Benchmarks

**Datasets and Metrics.** We further evaluate our approach on 3D question answering benchmarks. We evaluate on ScanQA [1] for 3D spatial reasoning and SQA3D [40] for situated reasoning, both built on ScanNet [13]. We follow the standard evaluation settings for each benchmark and use widely adopted metrics to assess answer quality. For ScanQA, we report exact match accuracy (EM), CIDEr, BLEU-4, METEOR, and ROUGE-L. For SQA3D, we evaluate performance using exact match accuracy (EM).

**Baselines.** We compare against models covering different input modalities and task specializations. Task-specific models ScanQA [1], SQA3D [40], and 3D-VisTA [76] are designed for 3D question answering. We compare against models that take 3D or 2.5D inputs and require additional modalities such as point clouds or depth maps, including Video-3D LLM [74], 3DRS [29], and Ross3D [48]. We further compare with video-only models such as SPAR [68] and VG-LLM [73], which, like ours, rely solely on video.

Table 4. **Evaluation on ScanQA [1] and SQA3D [40] for 3D understanding tasks.** “C” stands for “CIDEr”, “B-4” for “BLEU-4”, “M” for “METEOR”, “R” for “ROUGE”, and “EM-1” for top-1 exact match. **Bold** and underline denote the best-performing and second-best performing models in each category, respectively.

Methods	Video Input	ScanQA (val)					SQA3D (test)	
		C	B-4	M	R	EM-1	EM-1	
<i>Task-Specific Models</i>								
ScanQA [1]	<span style="color:red">✗</span>	<u>64.9</u>	10.1	13.1	33.3	<u>21.1</u>		<u>47.2</u>
SQA3D [40]	<span style="color:red">✗</span>	-	<u>11.2</u>	<u>13.5</u>	<u>34.5</u>	-		46.6
3D-VisTA [76]	<span style="color:red">✗</span>	<b>69.6</b>	<u>10.4</u>	<u>13.9</u>	<u>35.7</u>	<u>22.4</u>		<b>48.5</b>
<i>3D/2.5D-Input Models</i>								
3D-LLM [22]	<span style="color:red">✗</span>	69.4	12.0	14.5	35.7	20.5		-
Chat-3D v2 [25]	<span style="color:red">✗</span>	87.6	14.0	-	-	-		54.7
LL3DA [7]	<span style="color:red">✗</span>	76.8	13.5	15.9	37.3	-		-
ChatScene [26]	<span style="color:red">✗</span>	87.7	14.3	18.0	41.6	21.6		54.6
LLaVA-3D [75]	<span style="color:red">✗</span>	103.1	16.4	<u>20.8</u>	49.6	<u>30.6</u>		60.1
Video-3D LLM [74]	<span style="color:red">✗</span>	102.1	16.4	20.0	49.3	30.1		58.6
3DRS [29]	<span style="color:red">✗</span>	<u>104.8</u>	17.2	20.5	<u>49.8</u>	30.3		60.6
Ross3D [48]	<span style="color:red">✗</span>	<b>107.0</b>	<u>17.9</u>	<u>20.9</u>	<u>50.7</u>	<u>30.8</u>		<b>63.0</b>
<i>Video-Input Models</i>								
InternVL2-8B [9]	<span style="color:green">✓</span>	62.5	3.3	14.5	34.3	-		33.0
Qwen2-VL-7B [2]	<span style="color:green">✓</span>	53.9	3.0	11.4	29.3	-		46.5
Qwen2-VL-72B [2]	<span style="color:green">✓</span>	66.9	12.0	13.0	35.2	-		47.0
LLaVA-Video-7B [72]	<span style="color:green">✓</span>	88.7	3.1	17.7	44.6	-		48.5
Oryx-34B [38]	<span style="color:green">✓</span>	72.3	-	15.0	37.3	-		-
Spatial-MLLM-4B [54]	<span style="color:green">✓</span>	91.8	<u>14.8</u>	<u>18.4</u>	<u>45.0</u>	-		<u>55.9</u>
<b>VLM<sup>2</sup>-7B (Ours)</b>	<span style="color:green">✓</span>	<b>105.5</b>	<u>17.7</u>	<u>20.5</u>	<u>50.3</u>	<u>30.7</u>		<b>60.4</b>
<i>Improve</i> $\uparrow$		+13.7	+2.9	+2.1	+5.3	-		+4.5

**Results.** We present the quantitative results on the ScanQA and SQA3D benchmarks in Table 4. Our method achieves state-of-the-art performance among video-only models on both benchmarks and also significantly outperforms all task-specific models. Compared with approaches that leverage additional 3D or 2.5D inputs, while Ross3D achieves better performance than ours, it exploits extra point clouds to render BEV images for reconstructive supervision. Our approach surpasses other 3D/2.5D input models, such as Video-3D LLM and 3DRS. We attribute these gains to our model’s ability to explicitly resolve semantic-geometric misalignment when constructing 3D-aware representations from video. Our viewpoint-aware geometry alignment and adaptive 3D position injection jointly enforce coherent alignment between visual and geometry tokens, leading to view-consistent 3D-aware representations.

## 4.3 Ablation Studies

In this section, we conduct ablation studies on VSI-Bench [60], a video-based benchmark for spatial reasoning. We first analyze the overall impact of our key components, then examine the effectiveness of the 3D-aware representation, and finally study how the lengths of working and episodic memories affect long-horizon performance.

**Overall Component Analysis.** Our component ablation studies are summarized in Table 5. We establish a strong video-only baseline by fine-tuning LLaVA-NeXT-Video-7B [71] with the same language backbone, training schedule, and compute budget for all variants. Incorporating our 3D-aware representation into the baseline yields an average

**Table 5. Ablation of model components.** We evaluate the effect of 3D-aware representation, working memory, and episodic memory. Each module contributes complementary improvements, and combining all yields the best overall performance.

3D-Aware Rep.	Work. Mem.	Epis. Mem.	Avg.	Numerical Question		Multiple-Choice Question			
				Abs.	Dist.	Room Size	Rel. Dist.	Rel. Dir.	Route Plan
✗	✗	✗	55.2	43.3	62.4	62.1	67.8	40.2	
✓	✗	✗	63.8	52.9	67.5	65.6	84.8	48.5	
✓	✓	✗	65.9	56.3	68.3	67.3	86.2	51.3	
✓	✗	✓	66.1	57.7	68.6	67.6	85.9	50.5	
✓	✓	✓	<b>67.8</b>	<b>59.6</b>	<b>69.0</b>	<b>87.8</b>	<b>52.6</b>		

**Table 6. Ablation of 3D-aware representations.** We compare different 3D foundation models (VGTT [49], CUT3R [50],  $\pi^3$  [52]) and fusion strategies (*Concat-MLP*, *Cross-Attn*) for constructing 3D-aware representations. Based on  $\pi^3$  and *Cross-Attn*, our viewpoint-aware geometry alignment (VAGA) and adaptive 3D position injection (A3PI) achieve the best results.

Methods	Avg.	Numerical Question		Multiple-Choice Question			
		Abs.	Dist.	Room Size	Rel. Dist.	Rel. Dir.	Route Plan
<i>Baseline</i>							
LLaVA-NeXT-Video-SFT	55.2	43.3	62.4	62.1	67.8	40.2	
<i>Sem-Geo Fusion (Concat-MLP)</i>							
Baseline + VGTT	41.4	38.6	45.6	38.7	47.6	36.6	
Baseline + CUT3R	43.3	39.8	51.4	41.3	45.9	38.1	
Baseline + $\pi^3$	40.4	38.3	42.5	41.0	45.2	35.1	
<i>Sem-Geo Fusion (Cross-Attn)</i>							
Baseline + VGTT	60.2	51.0	63.9	61.4	81.8	42.7	
Baseline + CUT3R	59.4	50.2	63.1	62.8	79.3	41.8	
Baseline + $\pi^3$	61.0	51.9	64.7	63.1	81.9	43.3	
<i>VLM<sup>2</sup> (Ours)</i> [3D Foundation: $\pi^3$ ; Sem-Geo Fusion: Cross-Attn]							
Baseline + A3PI (w/o adapt.)	58.9	50.3	64.5	60.5	77.2	41.9	
Baseline + A3PI	61.6	52.3	65.3	63.7	82.1	44.7	
Baseline + VAGA	62.9	52.5	66.4	64.9	84.0	46.6	
Baseline + A3PI + VAGA	63.8	52.9	67.5	65.6	84.8	48.5	

of 8.6% accuracy gain. Building on this representation, introducing working memory or episodic memory brings additional gains of 2.1% and 2.3%, respectively. When both memory modules are combined, our full model achieves the best performance, improving by 4.0% over the 3D-aware representation and by 12.6% over the baseline. The benefit is particularly pronounced on tasks such as *Route Plan* (+ 12.4), which requires spatial structure awareness, highlighting the importance of an explicit memory mechanism. These findings suggest that both a view-consistent 3D-aware representation and a persistent dual-memory module are crucial components for advanced spatial reasoning.

**Effectiveness of 3D-Aware Representation.** We ablate the choice of 3D backbone and fusion strategy on top of the aforementioned video-based baseline, as shown in Table 6. To incorporate geometry tokens from 3D foundation models into visual tokens, we compare two fusion strategies. A simple *Concat-MLP* fusion, which concatenates 2D visual tokens with 3D geometry tokens and maps them with an MLP, yields lower performance (40.4–43.3), indicating that naïve concatenation leaves the semantic-geometric misalignment unresolved. Replacing *Concat-MLP* with a *Cross-Attn* fusion using 3D backbones (VGTT, CUT3R,

**Table 7. Ablation of dual-memory length.** We vary the length of working memory ( $L_w$ ) and episodic memory ( $L_e$ ) on VSI-Bench. The setting ( $L_w, L_e$ )=(8, 32) has the best overall performance.

Memory Size			VSI-Bench		
$L_w$	$L_e$		Numerical	Multiple-Choice	Avg.
4	8		64.1	58.5	61.3
8	8		65.6	66.9	66.3
8	16		67.1	67.4	67.3
8	32		<b>68.2</b>	<b>69.4</b>	<b>68.8</b>
16	8		65.2	65.7	65.5
16	16		67.3	67.9	67.6
16	32		67.9	68.6	68.3

$\pi^3$ ) raises performance to 59.4–61.0, showing that geometric cues help with a stronger fusion strategy but still fall short of our approach. Our viewpoint-aware geometry alignment (VAGA) with adaptive 3D position injection (A3PI) achieves the best accuracy, boosting performance from 61.0 to 63.8. Removing the adaptive mechanism from A3PI reduces the performance to 58.9, indicating that injecting position information into all visual tokens introduces noise in irrelevant regions and distorts feature distributions, highlighting the importance of adaptive injection.

**Ablation of Dual-Memory Length.** We study the effect of memory length by varying the working memory window  $L_w$  and episodic memory capacity  $L_e$ . As reported in Table 7, increasing episodic memory capacity  $L_e$  improves performance up to  $L_e = 32$ , highlighting the benefit of long-term memory. In contrast, a larger working memory window  $L_w$  is not always helpful. Working memory attends to recent frames, so having a short window may miss spatial cues needed to disambiguate nearby objects and layouts, whereas a long window introduces irrelevant tokens that dilute attention. We find that  $L_w = 8, L_e = 32$  achieves the best performance, best enabling our dual-memory design to effectively preserve persistent context for spatial reasoning.

## 5 Conclusion

In this paper, we propose  $VLM^2$ , a vision-language model for video-based spatial reasoning that addresses two critical challenges: semantic-geometric misalignment and the absence of persistent memory.  $VLM^2$  constructs a view-consistent 3D-aware representation from video by adaptively grounding visual features into 3D space and enforcing cross-view consistency, enabling coherent 3D understanding. On top of this representation, we introduce a dual-memory module that combines a sliding-window working memory for immediate context with a fixed-capacity episodic memory for long-term recall, allowing efficient long-horizon spatial reasoning. Extensive experiments across multiple spatial reasoning benchmarks demonstrate that our method achieves state-of-the-art performance, advancing the frontier of visual-spatial intelligence.

## References

[1] Daichi Azuma, Taiki Miyanishi, Shuhei Kurita, and Motoaki Kawanabe. Scanqa: 3d question answering for spatial scene understanding. In *proceedings of the IEEE/CVF conference on computer vision and pattern recognition*, pages 19129–19139, 2022. 2, 7, 13, 14

[2] Shuai Bai, Keqin Chen, Xuejing Liu, Jialin Wang, Wenbin Ge, Sibo Song, Kai Dang, Peng Wang, Shijie Wang, Jun Tang, et al. Qwen2. 5-vl technical report. *arXiv preprint arXiv:2502.13923*, 2025. 1, 2, 6, 7, 14, 15

[3] Gilad Baruch, Zhuoyuan Chen, Afshin Dehghan, Tal Dimry, Yuri Feigin, Peter Fu, Thomas Gebauer, Brandon Joffe, Daniel Kurz, Arik Schwartz, et al. Arkitscenes: A diverse real-world dataset for 3d indoor scene understanding using mobile rgb-d data. *arXiv preprint arXiv:2111.08897*, 2021. 5

[4] Wenxiao Cai, Iaroslav Ponomarenko, Jianhao Yuan, Xiaoqi Li, Wankou Yang, Hao Dong, and Bo Zhao. Spatialbot: Precise spatial understanding with vision language models. In *2025 IEEE International Conference on Robotics and Automation (ICRA)*, pages 9490–9498. IEEE, 2025. 3

[5] Jiazhong Cen, Xudong Zhou, Jiemin Fang, Changsong Wen, Lingxi Xie, Xiaopeng Zhang, Wei Shen, and Qi Tian. Tackling view-dependent semantics in 3d language gaussian splatting. *arXiv preprint arXiv:2505.24746*, 2025. 1

[6] Boyuan Chen, Zhuo Xu, Sean Kirmani, Brain Ichter, Dorsa Sadigh, Leonidas Guibas, and Fei Xia. Spatialvlm: Endowing vision-language models with spatial reasoning capabilities. In *Proceedings of the IEEE/CVF Conference on Computer Vision and Pattern Recognition*, pages 14455–14465, 2024. 1, 3

[7] Sijin Chen, Xin Chen, Chi Zhang, Mingsheng Li, Gang Yu, Hao Fei, Hongyuan Zhu, Jiayuan Fan, and Tao Chen. Ll3da: Visual interactive instruction tuning for omni-3d understanding reasoning and planning. In *Proceedings of the IEEE/CVF conference on computer vision and pattern recognition*, pages 26428–26438, 2024. 1, 2, 7

[8] Yiming Chen, Zekun Qi, Wenyao Zhang, Xin Jin, Li Zhang, and Peidong Liu. Reasoning in space via grounding in the world. *arXiv preprint arXiv:2510.13800*, 2025. 2

[9] Zhe Chen, Weiyun Wang, Yue Cao, Yangzhou Liu, Zhangwei Gao, Erfei Cui, Jinguo Zhu, Shenglong Ye, Hao Tian, Zhaoyang Liu, et al. Expanding performance boundaries of open-source multimodal models with model, data, and test-time scaling. *arXiv preprint arXiv:2412.05271*, 2024. 7

[10] Zhe Chen, Weiyun Wang, Hao Tian, Shenglong Ye, Zhangwei Gao, Erfei Cui, Wenwen Tong, Kongzhi Hu, Jiapeng Luo, Zheng Ma, et al. How far are we to gpt-4v? closing the gap to commercial multimodal models with open-source suites. *Science China Information Sciences*, 67(12):220101, 2024. 15

[11] Zhuoguang Chen, Minghui Qin, Tianyuan Yuan, Zhe Liu, and Hang Zhao. Long3r: Long sequence streaming 3d reconstruction. In *Proceedings of the IEEE/CVF International Conference on Computer Vision (ICCV)*, pages 5273–5284, 2025. 3

[12] An-Chieh Cheng, Hongxu Yin, Yang Fu, Qiushan Guo, Ruihan Yang, Jan Kautz, Xiaolong Wang, and Sifei Liu. Spatialrgpt: Grounded spatial reasoning in vision-language models. *Advances in Neural Information Processing Systems*, 37:135062–135093, 2024. 3

[13] Angela Dai, Angel X Chang, Manolis Savva, Maciej Halber, Thomas Funkhouser, and Matthias Nießner. Scannet: Richly-annotated 3d reconstructions of indoor scenes. In *Proceedings of the IEEE conference on computer vision and pattern recognition*, pages 5828–5839, 2017. 5, 7

[14] Jiajun Deng, Tianyu He, Li Jiang, Tianyu Wang, Feras Dayoub, and Ian Reid. 3d-llava: Towards generalist 3d llms with omni superpoint transformer. In *Proceedings of the Computer Vision and Pattern Recognition Conference*, pages 3772–3782, 2025. 1, 2

[15] Markos Diomataris, Nikolaos Gkanatsios, Vassilis Pitsikalis, and Petros Maragos. Grounding consistency: Distilling spatial common sense for precise visual relationship detection. In *Proceedings of the IEEE/CVF International Conference on Computer Vision*, pages 15911–15920, 2021. 1

[16] Zhiwen Fan, Jian Zhang, Renjie Li, Junge Zhang, Runjin Chen, Hezhen Hu, Kevin Wang, Huaizhi Qu, Dilin Wang, Zhicheng Yan, et al. Vlm-3r: Vision-language models augmented with instruction-aligned 3d reconstruction. *arXiv preprint arXiv:2505.20279*, 2025. 2, 3, 5, 6, 7, 13, 14, 15, 19, 20

[17] Chaoyou Fu, Yuhang Dai, Yongdong Luo, Lei Li, Shuhuai Ren, Renrui Zhang, Zihan Wang, Chenyu Zhou, Yunhang Shen, Mengdan Zhang, et al. Video-mme: The first-ever comprehensive evaluation benchmark of multi-modal llms in video analysis. In *Proceedings of the Computer Vision and Pattern Recognition Conference*, pages 24108–24118, 2025. 6

[18] Petko Georgiev, Ving Ian Lei, Ryan Burnell, Libin Bai, Anmol Gulati, Garrett Tanzer, Damien Vincent, Zhufeng Pan, Shibo Wang, et al. Gemini 1.5: Unlocking multi-modal understanding across millions of tokens of context. *arXiv:2403.05530*, 2024. 6

[19] Bo He, Hengduo Li, Young Kyun Jang, Menglin Jia, Xuefei Cao, Ashish Shah, Abhinav Shrivastava, and Ser-Nam Lim. Ma-lm: Memory-augmented large multimodal model for long-term video understanding. In *Proceedings of the IEEE/CVF Conference on Computer Vision and Pattern Recognition*, pages 13504–13514, 2024. 3

[20] Dan Hendrycks, Collin Burns, Steven Basart, Andy Zou, Mantas Mazeika, Dawn Song, and Jacob Steinhardt. Measuring massive multitask language understanding. *arXiv preprint arXiv:2009.03300*, 2020. 6

[21] Sepp Hochreiter and Jürgen Schmidhuber. Long short-term memory. *Neural computation*, 9(8):1735–1780, 1997. 2

[22] Yining Hong, Haoyu Zhen, Peihao Chen, Shuhong Zheng, Yilun Du, Zhenfang Chen, and Chuang Gan. 3d-llm: Injecting the 3d world into large language models. *Advances in Neural Information Processing Systems*, 36:20482–20494, 2023. 2, 7

[23] Edward J Hu, Yelong Shen, Phillip Wallis, Zeyuan Allen-Zhu, Yuanzhi Li, Shean Wang, Lu Wang, Weizhu Chen, et al. Lora: Low-rank adaptation of large language models. *ICLR*, 1(2):3, 2022. 5, 13

[24] Wenbo Hu, Yining Hong, Yanjun Wang, Leison Gao, Zibu Wei, Xingcheng Yao, Nanyun Peng, Yonatan Bitton, Idan Szpektor, and Kai-Wei Chang. 3dllum-mem: Long-term spatial-temporal memory for embodied 3d large language model. *arXiv preprint arXiv:2505.22657*, 2025. 2, 3

[25] Haifeng Huang, Zehan Wang, Rongjie Huang, Luping Liu, Xize Cheng, Yang Zhao, Tao Jin, and Zhou Zhao. Chat-3d v2: Bridging 3d scene and large language models with object identifiers. *CoRR*, 2023. 1, 2, 7

[26] Haifeng Huang, Yilun Chen, Zehan Wang, Rongjie Huang, Runsen Xu, Tai Wang, Luping Liu, Xize Cheng, Yang Zhao, Jiangmiao Pang, et al. Chat-scene: Bridging 3d scene and large language models with object identifiers. *Advances in Neural Information Processing Systems*, 37: 113991–114017, 2024. 2, 7, 14

[27] Jiangyong Huang, Silong Yong, Xiaojian Ma, Xiongkun Linghu, Puha Li, Yan Wang, Qing Li, Song-Chun Zhu, Baoxiong Jia, and Siyuan Huang. An embodied generalist agent in 3d world. *arXiv preprint arXiv:2311.12871*, 2023. 2

[28] Junchao Huang, Xinting Hu, Boyao Han, Shaoshuai Shi, Zhuotao Tian, Tianyu He, and Li Jiang. Memory forcing: Spatio-temporal memory for consistent scene generation on minecraft. *arXiv preprint arXiv:2510.03198*, 2025. 3

[29] Xiaohu Huang, Jingjing Wu, Qunyi Xie, and Kai Han. Mllms need 3d-aware representation supervision for scene understanding. *arXiv preprint arXiv:2506.01946*, 2025. 1, 3, 7, 13, 14

[30] Aaron Hurst, Adam Lerer, Adam P Goucher, Adam Perelman, Aditya Ramesh, Aidan Clark, AJ Ostrow, Akila Welihinda, Alan Hayes, Alec Radford, et al. Gpt-4o system card. *arXiv preprint arXiv:2410.21276*, 2024. 1, 6

[31] Mukul Khanna, Ram Ramrakhyta, Gunjan Chhablani, Sriram Yenamandra, Theophile Gervet, Matthew Chang, Zsolt Kira, Devendra Singh Chaplot, Dhruv Batra, and Roozbeh Mottaghi. Goat-bench: A benchmark for multi-modal lifelong navigation. In *Proceedings of the IEEE/CVF Conference on Computer Vision and Pattern Recognition*, pages 16373–16383, 2024. 3

[32] Yann LeCun. A path towards autonomous machine intelligence version 0.9. 2, 2022-06-27. *Open Review*, 62(1):1–62, 2022. 2

[33] Bo Li, Yuanhan Zhang, Dong Guo, Renrui Zhang, Feng Li, Hao Zhang, Kaichen Zhang, Peiyuan Zhang, Yanwei Li, Ziwei Liu, and Chunyuan Li. LLaVA-onevision: Easy visual task transfer. *TMLR*, 2025. 1, 2, 15

[34] Guibiao Liao, Kaichen Zhou, Zhenyu Bao, Kanglin Liu, and Qing Li. Ov-nerf: Open-vocabulary neural radiance fields with vision and language foundation models for 3d semantic understanding. *IEEE Transactions on Circuits and Systems for Video Technology*, 2024. 1

[35] Guibiao Liao, Jiankun Li, Zhenyu Bao, Xiaoqing Ye, Qing Li, and Kanglin Liu. Clip-gs: Clip-informed gaussian splatting for view-consistent 3d indoor semantic understanding. *ACM Transactions on Multimedia Computing, Communications and Applications*, 21(8):1–24, 2025. 1

[36] Ji Lin, Hongxu Yin, Wei Ping, Pavlo Molchanov, Mohammad Shoeybi, and Song Han. Vila: On pre-training for visual language models. In *CVPR*, 2024. 1, 15

[37] Yang Liu, Ming Ma, Xiaomin Yu, Pengxiang Ding, Han Zhao, Mingyang Sun, Siteng Huang, and Donglin Wang. Ssr: Enhancing depth perception in vision-language models via rationale-guided spatial reasoning. *arXiv preprint arXiv:2505.12448*, 2025. 1, 2

[38] Zuyan Liu, Yuhao Dong, Ziwei Liu, Winston Hu, Jiwen Lu, and Yongming Rao. Oryx mllm: On-demand spatial-temporal understanding at arbitrary resolution. *arXiv preprint arXiv:2409.12961*, 2024. 7, 14

[39] Wufei Ma, Haoyu Chen, Guofeng Zhang, Yu-Cheng Chou, Jieneng Chen, Celso de Melo, and Alan Yuille. 3dsrbench: A comprehensive 3d spatial reasoning benchmark. In *Proceedings of the IEEE/CVF International Conference on Computer Vision*, pages 6924–6934, 2025. 3

[40] Xiaojian Ma, Silong Yong, Zilong Zheng, Qing Li, Yitao Liang, Song-Chun Zhu, and Siyuan Huang. Sqa3d: Situated question answering in 3d scenes. *arXiv preprint arXiv:2210.07474*, 2022. 2, 7, 13, 14

[41] OpenAI. Gpt-4o, 2024. 2

[42] Samyam Rajbhandari, Jeff Rasley, Olatunji Ruwase, and Yuxiong He. Zero: Memory optimizations toward training trillion parameter models. In *SC20: International Conference for High Performance Computing, Networking, Storage and Analysis*, pages 1–16. IEEE, 2020. 13

[43] Jin-Chuan Shi, Miao Wang, Hao-Bin Duan, and Shao-Hua Guan. Language embedded 3d gaussians for open-vocabulary scene understanding. In *Proceedings of the IEEE/CVF Conference on Computer Vision and Pattern Recognition*, pages 5333–5343, 2024. 1

[44] Chan Hee Song, Valts Blukis, Jonathan Tremblay, Stephen Tyree, Yu Su, and Stan Birchfield. Robospatial: Teaching spatial understanding to 2d and 3d vision-language models for robotics. In *Proceedings of the Computer Vision and Pattern Recognition Conference*, pages 15768–15780, 2025. 3

[45] Enxin Song, Wenhao Chai, Guanhong Wang, Yucheng Zhang, Haoyang Zhou, Feiyang Wu, Haozhe Chi, Xun Guo, Tian Ye, Yanting Zhang, et al. Moviechat: From dense token to sparse memory for long video understanding. In *Proceedings of the IEEE/CVF Conference on Computer Vision and Pattern Recognition*, pages 18221–18232, 2024. 3

[46] Qwen Team et al. Qwen2 technical report. *arXiv preprint arXiv:2407.10671*, 2024. 5

[47] Hengyi Wang and Lourdes Agapito. 3d reconstruction with spatial memory. *arXiv preprint arXiv:2408.16061*, 2024. 3

[48] Haochen Wang, Yucheng Zhao, Tiancai Wang, Haoqiang Fan, Xiangyu Zhang, and Zhaoxiang Zhang. Ross3d: Constructive visual instruction tuning with 3d-awareness. *arXiv preprint arXiv:2504.01901*, 2025. 1, 2, 7, 13, 14

[49] Jianyuan Wang, Minghao Chen, Nikita Karaev, Andrea Vedaldi, Christian Rupprecht, and David Novotny. Vggt: Visual geometry grounded transformer. In *Proceedings of the Computer Vision and Pattern Recognition Conference*, pages 5294–5306, 2025. 2, 3, 8, 15

[50] Qianqian Wang, Yifei Zhang, Aleksander Holynski, Alexei A Efros, and Angjoo Kanazawa. Continuous 3d perception model with persistent state. In *Proceedings of the Computer Vision and Pattern Recognition Conference*, pages 10510–10522, 2025. 3, 5, 8, 15

[51] Shuzhe Wang, Vincent Leroy, Yohann Cabon, Boris Chidlovskii, and Jerome Revaud. Dust3r: Geometric 3d vision made easy. In *Proceedings of the IEEE/CVF Conference on Computer Vision and Pattern Recognition*, pages 20697–20709, 2024. 2

[52] Yifan Wang, Jianjun Zhou, Haoyi Zhu, Wenzheng Chang, Yang Zhou, Zizun Li, Junyi Chen, Jiangmiao Pang, Chunhua Shen, and Tong He.  $\pi^3$ : Scalable permutation-equivariant visual geometry learning. *arXiv preprint arXiv:2507.13347*, 2025. 3, 5, 8, 13, 15

[53] Zehan Wang, Haifeng Huang, Yang Zhao, Ziang Zhang, and Zhou Zhao. Chat-3d: Data-efficiently tuning large language model for universal dialogue of 3d scenes. *arXiv preprint arXiv:2308.08769*, 2023. 2

[54] Diankun Wu, Fangfu Liu, Yi-Hsin Hung, and Yueqi Duan. Spatial-mllm: Boosting mllm capabilities in visual-based spatial intelligence. *arXiv preprint arXiv:2505.23747*, 2025. 2, 3, 6, 7, 13, 14, 15

[55] Tong Wu, Shuai Yang, Ryan Po, Yinghao Xu, Ziwei Liu, Dahua Lin, and Gordon Wetzstein. Video world models with long-term spatial memory. *arXiv preprint arXiv:2506.05284*, 2025. 3

[56] Yuqi Wu, Wenzhao Zheng, Jie Zhou, and Jiwen Lu. Point3r: Streaming 3d reconstruction with explicit spatial pointer memory. *arXiv preprint arXiv:2507.02863*, 2025. 3

[57] Zhenjia Xu, Zhanpeng He, Jiajun Wu, and Shuran Song. Learning 3d dynamic scene representations for robot manipulation. *arXiv preprint arXiv:2011.01968*, 2020. 2

[58] Fuzhao Xue, Yukang Chen, Dacheng Li, Qinghao Hu, Ligeng Zhu, Xiuyu Li, Yunhao Fang, Haotian Tang, Shang Yang, Zhijian Liu, et al. Longvila: Scaling long-context visual language models for long videos. In *ICLR*, 2025. 15

[59] Jianwei Yang, Reuben Tan, Qianhui Wu, Ruijie Zheng, Baolin Peng, Yongyuan Liang, Yu Gu, Mu Cai, Seonghyeon Ye, Joel Jang, et al. Magma: A foundation model for multi-modal ai agents. In *Proceedings of the Computer Vision and Pattern Recognition Conference*, pages 14203–14214, 2025. 3

[60] Jihan Yang, Shusheng Yang, Anjali W Gupta, Rilyn Han, Li Fei-Fei, and Saining Xie. Thinking in space: How multimodal large language models see, remember, and recall spaces. In *Proceedings of the Computer Vision and Pattern Recognition Conference*, pages 10632–10643, 2025. 1, 2, 3, 5, 6, 7, 13, 14, 15, 16, 17, 18

[61] Rui Yang, Hanyang Chen, Junyu Zhang, Mark Zhao, Cheng Qian, Kangrui Wang, Qineng Wang, Teja Venkat Koripella, Marziyeh Movahedi, Manling Li, et al. Embodiedbench: Comprehensive benchmarking multi-modal large language models for vision-driven embodied agents. *arXiv preprint arXiv:2502.09560*, 2025. 3

[62] Yuncong Yang, Han Yang, Jiachen Zhou, Peihao Chen, Hongxin Zhang, Yilun Du, and Chuang Gan. 3d-mem: 3d scene memory for embodied exploration and reasoning. In *Proceedings of the Computer Vision and Pattern Recognition Conference*, pages 17294–17303, 2025. 2, 3

[63] Chandan Yeshwanth, Yueh-Cheng Liu, Matthias Nießner, and Angela Dai. Scannet++: A high-fidelity dataset of 3d indoor scenes. In *Proceedings of the IEEE/CVF International Conference on Computer Vision*, pages 12–22, 2023. 5

[64] Jiwen Yu, Jianhong Bai, Yiran Qin, Quande Liu, Xintao Wang, Pengfei Wan, Di Zhang, and Xihui Liu. Context as memory: Scene-consistent interactive long video generation with memory retrieval. *arXiv preprint arXiv:2506.03141*, 2025. 3

[65] Zhihao Yuan, Yibo Peng, Jinke Ren, Yinghong Liao, Yat-tong Han, Chun-Mei Feng, Hengshuang Zhao, Guanbin Li, Shuguang Cui, and Zhen Li. Empowering large language models with 3d situation awareness. In *Proceedings of the Computer Vision and Pattern Recognition Conference*, pages 19435–19445, 2025. 1

[66] Xiang Yue, Yuansheng Ni, Kai Zhang, Tianyu Zheng, Ruqi Liu, Ge Zhang, Samuel Stevens, Dongfu Jiang, Weiming Ren, Yuxuan Sun, et al. Mmmu: A massive multi-discipline multimodal understanding and reasoning benchmark for expert agi. In *Proceedings of the IEEE/CVF Conference on Computer Vision and Pattern Recognition*, pages 9556–9567, 2024. 6

[67] Haoji Zhang, Yiqin Wang, Yansong Tang, Yong Liu, Jiashi Feng, Jifeng Dai, and Xiaojie Jin. Flash-vstream: Memory-based real-time understanding for long video streams. *arXiv preprint arXiv:2406.08085*, 2024. 3

[68] Jiahui Zhang, Yurui Chen, Yanpeng Zhou, Yueming Xu, Ze Huang, Jilin Mei, Junhui Chen, Yu-Jie Yuan, Xinyue Cai, Guowei Huang, et al. From flatland to space: Teaching vision-language models to perceive and reason in 3d. *arXiv preprint arXiv:2503.22976*, 2025. 6, 7

[69] Kaichen Zhang, Bo Li, Peiyuan Zhang, Fanyi Pu, Joshua Adrian Cahyono, Kairui Hu, Shuai Liu, Yuanhan Zhang, Jingkang Yang, Chunyuan Li, et al. Lmms-eval: Reality check on the evaluation of large multimodal models. In *Findings of the Association for Computational Linguistics: NAACL 2025*, pages 881–916, 2025. 13

[70] Peiyuan Zhang, Kaichen Zhang, Bo Li, Guangtao Zeng, Jingkang Yang, Yuanhan Zhang, Ziyue Wang, Haoran Tan, Chunyuan Li, and Ziwei Liu. Long context transfer from language to vision. *arXiv:2406.16852*, 2024. 15

[71] Yuanhan Zhang, Bo Li, haotian Liu, Yong jae Lee, Liangke Gui, Di Fu, Jiashi Feng, Ziwei Liu, and Chunyuan Li. Llava-next: A strong zero-shot video understanding model, 2024. 1, 2, 6, 7, 15

[72] Yuanhan Zhang, Jimming Wu, Wei Li, Bo Li, Zejun Ma, Ziwei Liu, and Chunyuan Li. Video instruction tuning with synthetic data. *arXiv preprint arXiv:2410.02713*, 2024. 2, 3, 5, 7, 13, 14

[73] Duo Zheng, Shijia Huang, Yanyang Li, and Liwei Wang. Learning from videos for 3d world: Enhancing mllms with 3d vision geometry priors. *arXiv preprint arXiv:2505.24625*, 2025. 2, 3, 6, 7, 15

[74] Duo Zheng, Shijia Huang, and Liwei Wang. Video-3d llm: Learning position-aware video representation for 3d scene

understanding. In *Proceedings of the Computer Vision and Pattern Recognition Conference*, pages 8995–9006, 2025. 1, 2, 3, 7, 13, 14

[75] Chenming Zhu, Tai Wang, Wenwei Zhang, Jiangmiao Pang, and Xihui Liu. Llava-3d: A simple yet effective pathway to empowering lmms with 3d-awareness. *arXiv preprint arXiv:2409.18125*, 2024. 2, 7, 14

[76] Ziyu Zhu, Xiaojian Ma, Yixin Chen, Zhidong Deng, Siyuan Huang, and Qing Li. 3d-vista: Pre-trained transformer for 3d vision and text alignment. In *Proceedings of the IEEE/CVF International Conference on Computer Vision*, pages 2911–2921, 2023. 7, 14

[77] Ziyu Zhu, Xilin Wang, Yixuan Li, Zhuofan Zhang, Xiaojian Ma, Yixin Chen, Baoxiong Jia, Wei Liang, Qian Yu, Zhi-dong Deng, et al. Move to understand a 3d scene: Bridging visual grounding and exploration for efficient and versatile embodied navigation. In *Proceedings of the IEEE/CVF International Conference on Computer Vision*, pages 8120–8132, 2025. 3

# Vision-Language Memory for Spatial Reasoning

## Supplementary Material

### A Implementation Details

#### A.1 Training Datasets

Our VLM<sup>2</sup> is a spatial reasoning model capable of solving multiple spatial tasks. To achieve this capability, we construct a meticulously curated mixed dataset that combines spatial reasoning, spatial-temporal reasoning, and 3D scene understanding question-answering (QA) pairs.

**Spatial Reasoning QA.** We first include spatial reasoning datasets from VLM-3R [16], which focus on visual-spatial intelligence from egocentric videos. These QA pairs cover object count, absolute distance, object size, room size, relative distance, relative direction, and appearance order.

**Spatial-Temporal Reasoning QA.** To advance spatial-temporal reasoning in 3D environments, we further incorporate the spatial-temporal QA pairs from VLM-3R [16]. These questions interrogate camera dynamics, object states, and complex camera-object interactions over time, encompassing camera displacement, camera-object absolute distance, camera-object relative distance, object-object relative position, and camera movement direction.

**3D Scene Understanding QA.** We also include 3D scene understanding datasets from ScanQA [1] and SQA3D [40]. ScanQA provides 23K QA pairs about object alignment, directions, and object localization. SQA3D contributes approximately 79K situated QA pairs, where an agent in a 3D scene needs to infer and localize its situation (position, orientation, *etc.*) from textual descriptions, and then answer questions that require strong situated spatial reasoning. Together, these datasets enable VLM<sup>2</sup> to learn both video-based spatial reasoning and 3D scene understanding.

#### A.2 Training Details

Our model is built on LLaVA-Video-7B [72], initialized from the pretrained checkpoint *LLaVA-Video-7B-Qwen2*. The vision encoder is initialized with *siglipso400m-patch14-384*, and we adopt  $\pi^3$  [52] as the 3D foundation model. During training, both the vision encoder and the 3D foundation model are kept frozen, while the language backbone and our modules are updated. We set the gradient accumulation steps to 8, use the AdamW optimizer with a global batch size of 128 and a peak learning rate of 1e-5 for the LLM during the warmup phase, and uniformly sample 32 frames per scene for video-based input. For finetuning, we apply Low-Rank Adaptation (LoRA [23]) with a rank of 128 and a scaling factor of 256, and employ DeepSpeed ZeRO-2 [42] for memory optimization. All experiments are conducted on 8 NVIDIA H200 GPUs.

#### A.3 Evaluation Details

To assess the spatial reasoning capability of VLM<sup>2</sup> across a diverse set of tasks, we evaluate it on four widely adopted benchmarks. We conduct all evaluations using the LLMs-Eval [69] project. For video-based benchmarks, we uniformly sample 32 frames per scene from the input video.

**VSI-Bench.** We use VSI-Bench [60] to evaluate the model’s spatial reasoning performance from egocentric videos. We follow the official evaluation protocol of VSI-Bench, adopting a greedy decoding strategy for all models to ensure fair comparison. Moreover, we keep the question templates, prompt formats, and task-specific instructions exactly the same as in the original benchmark.

**VSTI-Bench.** To further assess how spatial reasoning evolves over time, we evaluate our model on VSTI-Bench [16], which focuses on spatial-temporal reasoning in egocentric video scenarios. We follow the same evaluation settings as VLM-3R [16], including task definitions, prompt formats, and decoding configurations.

**ScanQA and SQA3D.** For 3D scene understanding, we also evaluate on ScanQA [1] and SQA3D [40]. During inference, we set the number of frames to 32, following the evaluation configuration of Video-3D LLM [74], so as to maintain a comparable video context across methods.

### B Additional Experimental Results

#### B.1 Additional Results on ScanQA and SQA3D

Table 8 and Table 9 present additional evaluation results on the ScanQA [1] and SQA3D [40] benchmarks, complementing the results reported in the main paper.

**ScanQA.** VLM<sup>2</sup> shows strong performance on ScanQA, consistently outperforming all video-input models, including LLaVA-Video-7B [72] and Spatial-MLLM [54]. Although our method only takes video frames as input, it remains highly competitive against 3D/2.5D-input models that explicitly leverage depth or point clouds. These results indicate that our 3D-aware representation provides effective geometric cues for 3D scene understanding.

**SQA3D.** We also report SQA3D results broken down by six question types (*What, Is, How, Can, Which, Others*). As shown in Table 9, VLM<sup>2</sup> performs strongly among video-input models and remains competitive against methods that leverage additional 3D or 2.5D inputs. While Ross3D [48] achieves higher overall performance than ours, it exploits extra point clouds to render BEV images for reconstructive supervision. Our method surpasses other 3D/2.5D-input models such as Video-3D LLM [74] and 3DRS [29], demonstrating solid overall performance on SQA3D.

Table 8. **Additional evaluation results on ScanQA [1] for 3D understanding tasks.** **Bold** and underline denote the best-performing and second-best performing models in each category, respectively.

Methods	Video Input	ScanQA (val)							
		EM-1	BLEU-1	BLEU-2	BLEU-3	BLEU-4	ROUGE-L	METEOR	CIDEr
<i>Task-Specific Models</i>									
ScanQA [1]	✗	<u>21.1</u>	30.2	20.4	15.1	<u>10.1</u>	<u>33.3</u>	<u>13.1</u>	<u>64.9</u>
3D-VisTA [76]	✗	<b>22.4</b>	-	-	-	<b>10.4</b>	<b>35.7</b>	<b>13.9</b>	<b>69.6</b>
<i>3D/2.5D-Input Models</i>									
ChatScene [26]	✗	21.6	43.2	29.1	20.6	14.3	41.6	18.0	87.7
LLaVA-3D [75]	✗	27.0	-	-	-	14.5	<u>50.1</u>	<u>20.7</u>	91.7
Video-3D LLM [74]	✗	30.1	47.1	31.7	22.8	16.2	49.0	19.8	102.1
3DRS [29]	✗	<u>30.3</u>	<u>48.4</u>	<u>32.7</u>	<u>23.8</u>	<u>17.2</u>	49.8	20.5	<u>104.8</u>
Ross3D [48]	✗	<b>30.8</b>	<b>49.2</b>	<b>33.7</b>	<b>24.9</b>	<b>17.9</b>	<b>50.7</b>	<b>20.9</b>	<b>107.0</b>
<i>Video-Input Models</i>									
Qwen2-VL-7B [2]	✓	19.0	27.8	13.6	6.3	3.0	29.3	11.4	53.9
Qwen2-VL-72B [2]	✓	24.0	26.8	17.8	14.6	12.0	35.2	13.0	66.9
LLaVA-Video-7B [72]	✓	-	39.7	26.6	9.3	3.1	44.6	17.7	88.7
Oryx-34B [38]	✓	-	38.0	24.6	-	-	37.3	15.0	72.3
Spatial-MLLM-4B [54]	✓	<u>26.3</u>	<u>44.4</u>	<u>28.8</u>	<u>21.9</u>	<u>14.8</u>	<u>45.0</u>	<u>18.4</u>	<u>91.8</u>
<b>VLM<sup>2</sup>-7B (Ours)</b>	✓	<b>30.7</b>	<b>48.7</b>	<b>33.1</b>	<b>24.5</b>	<b>17.7</b>	<b>50.3</b>	<b>20.5</b>	<b>105.5</b>

Table 9. **Additional evaluation results on SQA3D [40] for 3D understanding tasks.** **Bold** and underline denote the best-performing and second-best performing models in each category, respectively.

Methods	Video Input	SQA3D (test)						Avg.
		What	Is	How	Can	Which	Others	
<i>Task-Specific Models</i>								
SQA3D [40]	✗	<u>31.6</u>	<b>63.8</b>	<b>46.0</b>	<u>69.5</u>	<u>43.9</u>	<u>45.3</u>	<u>46.6</u>
3D-VisTA [76]	✗	<b>34.8</b>	<u>63.3</u>	<u>45.4</u>	<b>69.8</b>	<b>47.2</b>	<b>48.1</b>	<b>48.5</b>
<i>3D/2.5D-Input Models</i>								
ChatScene [26]	✗	45.4	67.0	52.0	69.5	49.9	55.0	54.6
LLaVA-3D [75]	✗	-	-	-	-	-	-	55.6
Video-3D LLM [74]	✗	51.1	72.4	55.5	69.8	<u>51.3</u>	56.0	58.6
3DRS [29]	✗	<u>54.4</u>	<u>75.2</u>	<u>57.0</u>	<b>72.2</b>	49.9	<u>59.0</u>	<u>60.6</u>
Ross3D [48]	✗	<b>56.0</b>	<b>79.8</b>	<b>60.6</b>	<u>70.4</u>	<b>55.3</b>	<b>60.1</b>	<b>63.0</b>
<i>Video-Input Models</i>								
Qwen2-VL-7B [2]	✓	39.7	56.6	41.1	55.9	47.6	47.2	46.5
Qwen2-VL-72B [2]	✓	41.7	56.3	41.5	55.6	44.5	48.0	47.0
LLaVA-Video-7B [72]	✓	42.7	56.3	47.5	55.3	50.1	47.2	48.5
Spatial-MLLM-4B [54]	✓	<u>45.9</u>	<u>71.6</u>	<u>55.1</u>	<b>69.5</b>	<b>52.0</b>	<u>53.0</u>	<u>55.9</u>
<b>VLM<sup>2</sup>-7B (Ours)</b>	✓	<b>54.5</b>	<b>74.8</b>	<b>58.1</b>	<u>68.1</u>	<u>51.6</u>	<b>58.7</b>	<b>60.4</b>

Overall, these supplementary results show that VLM<sup>2</sup> is effective not only on video-based spatial reasoning benchmarks but also on 3D scene understanding tasks such as ScanQA and SQA3D, achieving strong performance across a broad range of evaluation settings and benchmarks.

## B.2 Additional Long-Horizon Reasoning Results

Table 10 reports additional long-horizon spatial reasoning results on VSI-Bench [60] and VSTI-Bench [16], complementing the comparisons in the main paper. We follow the same evaluation protocol and video-length partitioning

as in Table 3, where videos are grouped into Short (< 1 min), Mid (1–2 min), and Long (> 2 min). For Spatial-MLLM [54], the original setting uses 16 input frames for evaluation. We also include a 32-frame variant (marked with \*) to ensure a consistent input setting across methods.

## B.3 Additional Ablations on Sem-Geo Fusion

In Table 6 of the main paper, we compared two semantic-geometric (Sem-Geo) fusion strategies: *Concat-MLP* and *Cross-Attn*. Here, we provide additional ablations by including the *Add* fusion variant, which performs simple

Table 10. **Additional long-horizon spatial reasoning results on VSI-Bench [60] and VSTI-Bench [16].** Videos are grouped into Short (< 1 min), Mid (1–2 min), and Long (> 2 min). For Spatial-MLLM [54], the original setting uses 16 input frames for evaluation, while methods marked with \* correspond to a 32-frame input setting, used to ensure a consistent frame setting across methods.

Methods	VSI-Bench				VSTI-Bench			
	Avg.	Short	Mid	Long	Avg.	Short	Mid	Long
<i>Open-sourced VLMs</i>								
LongVA-7B [70]	31.1	33.5	32.2	28.8	38.2	36.9	38.4	40.5
InternVL2-8B [10]	34.6	35.8	33.8	34.9	49.1	46.2	49.9	53.3
InternVL2-40B [10]	36.1	38.5	36.0	35.1	50.3	46.0	51.6	56.2
LongVILA-8B [58]	21.2	20.1	21.0	21.9	34.3	34.6	33.9	34.7
VILA-1.5-8B [36]	30.7	35.1	31.9	27.4	40.9	39.8	42.1	40.6
VILA-1.5-40B [36]	31.6	33.3	32.3	30.1	44.8	41.9	45.1	50.0
Qwen2.5VL-7B [2]	29.5	34.3	28.3	28.4	45.9	43.3	48.4	45.5
Qwen2.5VL-72B [2]	36.3	39.2	36.6	34.7	49.4	45.1	50.8	55.2
LLaVA-OneVision-7B [33]	34.1	38.2	34.3	32.0	46.6	44.1	47.6	49.8
LLaVA-OneVision-72B [33]	41.2	43.0	41.5	40.2	52.2	48.2	52.9	59.2
LLaVA-NeXT-Video-7B [71]	36.8	38.5	37.3	35.5	46.4	43.0	47.9	50.1
LLaVA-NeXT-Video-72B [71]	41.1	41.3	40.7	41.4	51.3	47.6	51.9	57.6
<i>Spatial-Enhanced Models</i>								
Spatial-MLLM-4B [54]	48.1	49.8	48.3	47.2	-	-	-	-
Spatial-MLLM-4B* [54]	49.0	49.7	49.3	48.5	-	-	-	-
VG-LLM-4B [73]	47.4	49.1	48.7	45.2	-	-	-	-
VG-LLM-8B [73]	50.5	51.9	49.7	50.6	-	-	-	-
VLM-3R-7B [16]	63.2	67.1	64.7	60.0	63.6	61.1	64.7	66.4
<b>VLM<sup>2</sup>-7B (Ours)</b>	<b>69.4</b>	<b>71.0</b>	<b>70.0</b>	<b>68.1</b>	<b>69.5</b>	<b>65.9</b>	<b>70.6</b>	<b>74.6</b>
<i>Improve</i> $\uparrow$	<b>+6.2</b>	+3.9	+5.3	+8.1	<b>+5.9</b>	+4.8	+5.9	+8.2

Table 11. **Additional ablations of Sem-Geo fusion strategies.** In addition to *Concat-MLP* and *Cross-Attn* reported in the main paper, we further include the *Add* variant under three representative 3D foundation models (VGTT [49], CUT3R [50],  $\pi^3$  [52]).

Methods	Avg.	Numerical Question		Multiple-Choice Question		
		Abs. Dist.	Room Size	Rel. Dist.	Rel. Dir.	Route Plan
<i>Baseline</i>						
LLaVA-NeXT-Video-SFT	55.2	43.3	62.4	62.1	67.8	40.2
<i>Sem-Geo Fusion (Concat-MLP)</i>						
Baseline + VGTT	41.4	38.6	45.6	38.7	47.6	36.6
Baseline + CUT3R	43.3	39.8	51.4	41.3	45.9	38.1
Baseline + $\pi^3$	40.4	38.3	42.5	41.0	45.2	35.1
<i>Sem-Geo Fusion (Cross-Attn)</i>						
Baseline + VGTT	60.2	<u>51.0</u>	63.9	61.4	<u>81.8</u>	42.7
Baseline + CUT3R	59.4	50.2	63.1	62.8	79.3	41.8
Baseline + $\pi^3$	<b>61.0</b>	<b>51.9</b>	<b>64.7</b>	<u>63.1</u>	<b>81.9</b>	<b>43.3</b>
<i>Sem-Geo Fusion (Add)</i>						
Baseline + VGTT	59.9	50.5	64.1	61.3	81.6	42.3
Baseline + CUT3R	58.5	47.4	<b>64.7</b>	62.5	75.9	41.8
Baseline + $\pi^3$	60.7	50.9	<u>64.2</u>	<b>63.8</b>	81.5	<u>42.9</u>

element-wise addition between semantic and geometric features. Table 11 reports the full comparison across all three fusion strategies. We follow exactly the same training and evaluation setups as in the main experiments. These supplementary results further confirm the consistent trends reported in the main paper:  $\pi^3$  consistently provides the

strongest geometric prior, and *Cross-Attn* remains the most effective Sem-Geo fusion strategy among all variants.

## C Qualitative Results

Figures 3 to 7 show qualitative examples of VLM<sup>2</sup> on the VSI-Bench [60] and VSTI-Bench [16] benchmarks. We include cases covering various spatial reasoning tasks, such as configurational estimation, measurement estimation, and temporal reasoning. These visual examples illustrate the model’s spatial reasoning capability across different tasks.

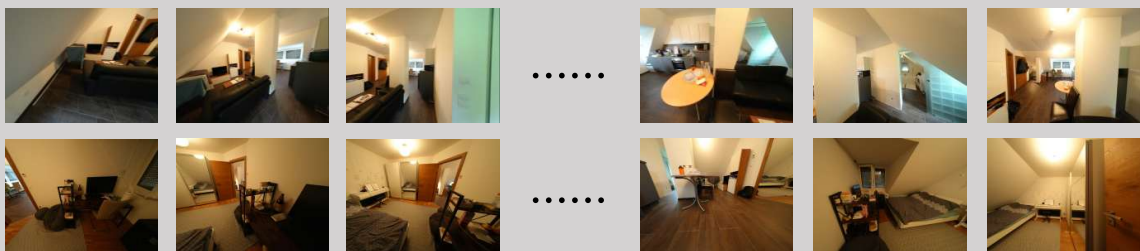
## Video



**Question:** How many chair(s) are in this room?

**Answer:** 6

## Video



**Question:** Mearsuring from the closest point of each object, what is the distance between the bed and the sofa (in meters)?

**Answer:** 3.2

## Video



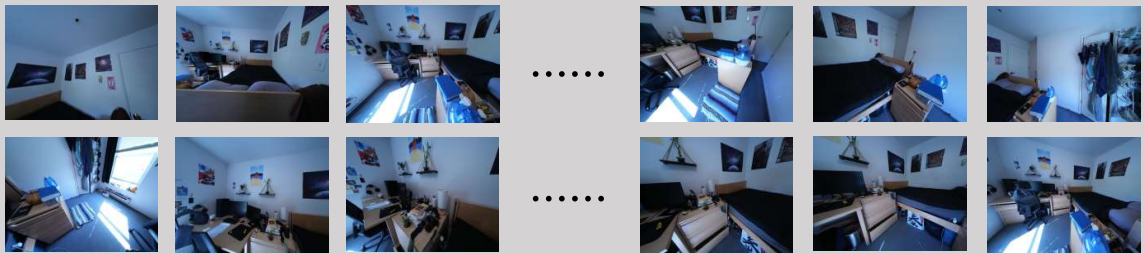
**Question:** You are a robot beginning at the kitchen sink and facing window. You want to navigate to the refrigerator. You will perform the following actions (Note: for each [please fill in], choose either 'turn back,' 'turn left,' or 'turn right.'): 1. [please fill in] 2. Go forward until the refrigerator. You have reached the final destination.

**Options:** A. Turn Back B. Turn Right C. Turn Left

**Answer:** A

Figure 3. Qualitative examples on VSI-Bench [60].

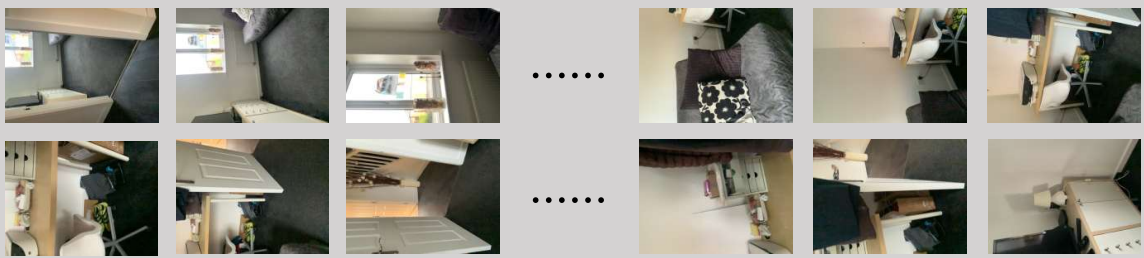
### Video



**Question:** What is the size of this room (in square meters)? If multiple rooms are shown, estimate the size of the combined space.

**Answer:** 10.5

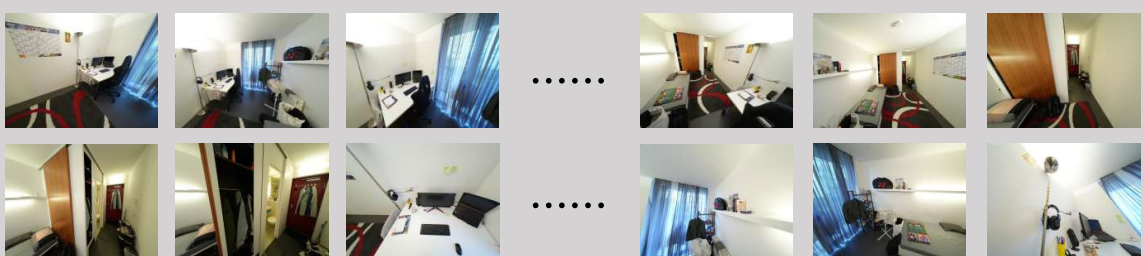
### Video



**Question:** What is the length of the longest dimension (length, width, or height) of the chair; measured in centimeters?

**Answer:** 69

### Video

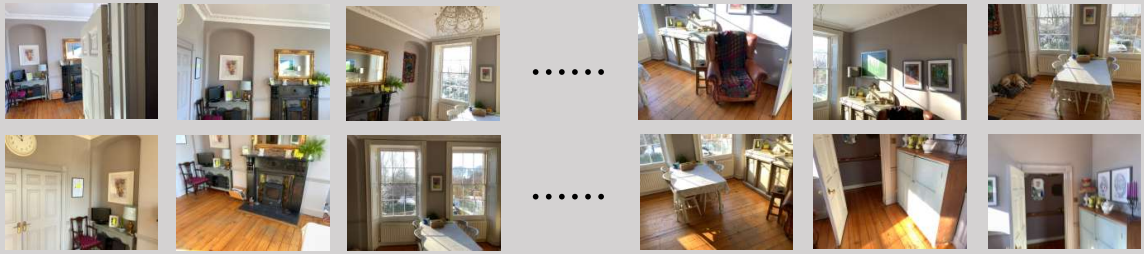


**Question:** What will be the first-time appearance order of the following categories in the video: basket, door, pillow, laptop? Options: A. basket, pillow, door, laptop B. pillow, door, laptop, basket C. basket, door, pillow, laptop D. door, basket, pillow, laptop

**Answer:** B

Figure 4. Qualitative examples on VSI-Bench [60].

## Video



**Question:** Measuring from the closest point of each object, which of these objects (chair, table, tv, fireplace) is the closest to the sofa? Options: A. chair B. table C. tv D. fireplace

**Answer:** B

## Video



**Question:** If I am standing by the computer tower and facing the heater, is the door to my left, right, or back? An object is to my back if I would have to turn at least 135 degrees in order to face it. Options: A. back B. right C. left

**Answer:** A

## Video



**Question:** If I am standing by the ceiling light and facing the door, is the kettle to my front-left, front-right, back-left, or back-right? The directions refer to the quadrants of a Cartesian plane (if I am standing at the origin and facing along the positive y-axis). Options: A. front-left B. back-right C. front-right D. back-left

**Answer:** D

Figure 5. Qualitative examples on VSI-Bench [60].

## Video

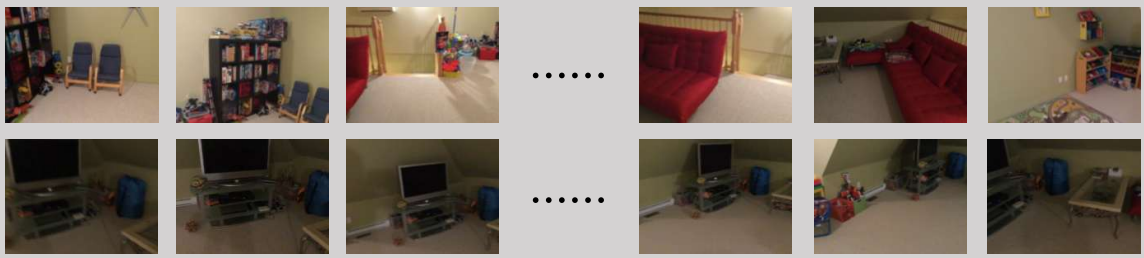


**Question:** Measuring from the closest point of each object, which of these objects (plant, window) is the closest to the camera in frame 4 of 32? Options: A. plant B. window

**Answer:** B

---

## Video



**Question:** During the sequence between frame 4 and frame 23 of 32, what was the primary consistent direction of the camera's movement relative to its orientation at the start? The options are Forward, Left, and Right.

Options: A. Forward B. Left C. Right

**Answer:** C

---

## Video

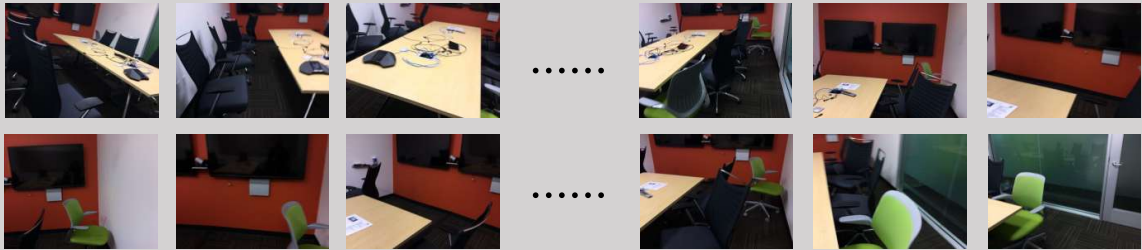


**Question:** What is the approximate distance (in meters) between the camera (or the person filming) and the nearest point of the backpack in frame 10 of 32?

**Answer:** 0.7

Figure 6. Qualitative examples on VSTI-Bench [16].

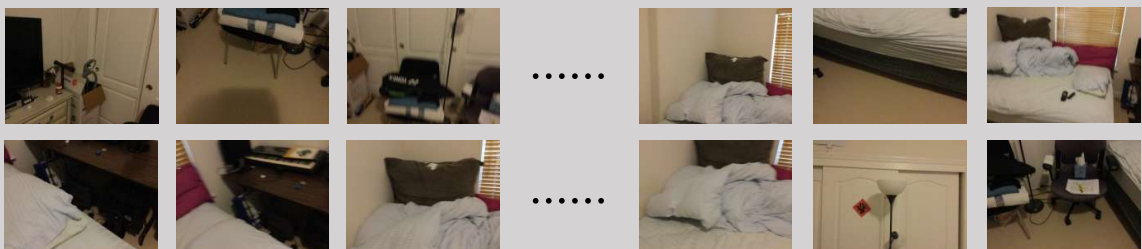
### Video



**Question:** Approximately how far (in meters) did the camera move between frame 24 and frame 31 of 32?

**Answer:** 1.2

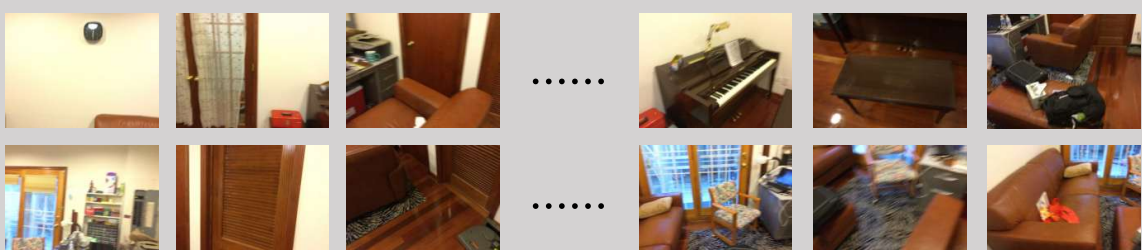
### Video



**Question:** In frame 13 of 31, relative to monitor, is bed to the [Left/Right]? Options: A. Right B. Left

**Answer:** B

### Video



**Question:** In frame 1 of 31, relative to clock, is piano to the [Up/Down]? Options: A. Down B. Up

**Answer:** A

Figure 7. Qualitative examples on VSTI-Bench [16].